Synthesis of Titanium Dioxide Nanotubes from Titanium Dioxide Nanoparticles and Their Photocatalytic Activities

Rungnapa Tongpool*, Saowaluk Chaleawlert-umpon and Sorachon Yoriya

National Metal and Materials Technology Centre (MTEC) 114, Paholyothin Rd., Klong 1, Klong Luang, Pathumthani 12120, Thailand

*Corresponding author. E-mail: rungnapt@mtec.or.th

ABSTRACT

Titanium dioxide nanotubes (TiNT) were prepared by treating titanium dioxide (TiO$_2$) nanoparticles with hot NaOH solution. The TiO$_2$ nanoparticles (anatase) used in this work were precipitated TiO$_2$, SiO$_2$-TiO$_2$ and commercial-grade (C02 and P25) nanoparticles. The diameters of the obtained nanotubes were nearly the same (~5-16 nm), regardless of the type of the starting nanoparticles. The photocatalytic actitivity of TiO$_2$ samples were dependent on their crystallinity, defects on the surface, photon absorptivity, particle size and surface area being exposed to UV radiation. TiNT had higher surface areas and more surface defects than the starting particles but the crystallinity, photon absorptivity and photocatalytic activities of the former were lower than those of the latter. The precipitated TiO$_2$ nanoparticles showed highest photocatalytic activity in KI oxidation, while TiNT from SiO$_2$-TiO$_2$ particles showed lowest activity. For an equal amount of absorbed photon, SiO$_2$-TiO$_2$ particles showed highest photon-to-product conversion efficiency.

Key words: Titanium dioxide, Nanoparticles, Nanotubes, SiO$_2$-TiO$_2$, Photocatalysis

INTRODUCTION

TiO$_2$ nanoparticles are used in many applications, including dye-sensitized solar cells (Kay and Gratzel, 1996; Adachi et al., 2003), photocatalytic reactions (Wilke and Breuer, 1999; Yang et al., 2002) and water purification systems (Horton and Garrett, 2002; Carmignani and Frederick, 2003) due to their high surface area and photocatalytic activity. TiO$_2$ nanoparticles can be obtained by various ways, including vapor deposition, precipitation and sol-gel method (Kasuka and Hiramatzu, 1998, 2000, 2003). It has been reported that surface area of the nanoparticles can be increased by treating with NaOH to form TiNT (Kasuka and Hiramatzu, 1998, 2000, 2003).The TiNT formation involves exfoliation of the crystalline particles into layered crystalline sheets and folding of the sheet-like structure (Tian et al., 2003; Yao et al., 2003). Both sides of the single-layer sheets have dangling bonds. Rolling of the sheets to form tubes reduces the number of dangling bonds and thus, the surface energy. The TiNT can also be synthesised using a template (Hoyer, 1996; Jung et

al., 2002; Adachi et al., 2003). SiO_2-TiO_2 was reported to show higher surface area than that of pure TiO_2. Moreover, TiNT was found coexisted with the nanoparticles in the samples having 5 at.% Si (Zhang and Reller, 2002).

TiNT can be used as a novel filter, a novel functional material where organic or inorganic materials are inserted, a magnetic substance where magnetic materials are inserted inside the tube (Kasuka and Hiramatzu, 1998, 2000, 2003). Xu et al., (2005) used Zn-doped TiNT, synthesized via an assembly process, as photocatalyst. There have been no reports on the photocatalytic activity of TiNT, synthesized from TiO_2 nanoparticles and compared its activity with its starting particles. In this work, TiNT was obtained by treating TiO_2 nanoparticles with hot NaOH solution. The differences in photocatalytic activities of TiNT and their starting particles are explained in terms of morphology, crystallinity, surface area and photon absorptivity.

MATERIALS AND METHODS

Material preparation

TiO_2 nanoparticles were precipitated from hydrolysis reaction of tetraisopropyl orthotitanate (Ti(OiPr)$_4$, Fluka) and calcined at 450°C for 1 h. The sol-gel SiO_2-TiO_2 was prepared as described by Kasuga et al. (1998). The reagents used were Ti(OiPr)$_4$, tetraethylorthosilicate (TEOS, 98%, Fluka), ethanol (99.9%, Mallinckrodt) and hydrochloric acid (HCl, 37%, Lab Scan). The gel was calcined at 450°C for 2 h to obtain SiO_2-TiO_2 particles containing 20 mol% of SiO_2 and 80 mol% of TiO_2. The powder of precipitated TiO_2, sol-gel derived SiO_2-TiO_2 and commercial TiO_2 (C02, Smith supply, Thailand, no. 02) were treated with 10 M NaOH at 110°C for 20 h in closed containers to obtain TiNT (Kasuga et al., 1998). The obtained nanotubes were washed with 0.1 M HCl and distilled water until the washing water showed pH 7. Some of the TiNT were reheated at 450°C for 2 h to increase the crystallinity.

Analysis and characterization

Structural properties of the samples were examined by an X-ray diffractrometer (XRD, JEOL JDX-3530). Scanning electron microscope (JEOL JSM-6301F with OXFORD ISIS 300 energy-dispersive spectroscopy) and transmission electron microscope (JEOL JEM 1220) were used to investigate the size of the samples. Surface area of the samples was obtained by BET surface area analysis, using surface area analyzer (Micromeritics FlowSorb II 2300) and the method followed ISO 9277. P25 TiO_2 (J.J. Degussa) was also characterised. The presence of Si-O-Si bond in the SiO_2-TiO_2 particles and nanotubes was investigated by fourier-transform infrared spectroscopy (FTIR)(Perkin Elmer System 2000).

Photocatalytic activity

The photocatalytic activity of TiO_2 samples was measured through the oxidation of I- to I_3^- in the excess iodide conditions as follow: 0.05 g of TiO_2 samples including P25 were added into 10 ml of 0.2 M KI aqueous solution. They were

exposed to UV light of 366 nm (Minerallight light UVGL-58) for 15, 30, 45 and 60 min. The KI solution (colorless) was decomposed to I_3^- (yellow) under the UV exposure. The suspensions were filtered and diluted 5 times. Then the absorbance of the clear solutions was measured, using UV-Visible spectrometer (JASCO V-530).

RESULTS AND DISCUSSION

XRD patterns (Figs. 1a and 1b) showed that most of the TiO_2 samples consisted of 100% anatase crystal form. Only P25 and those obtained from SiO_2-TiO_2 contained a small amount of rutile phase. The degree of crystallinity of the synthesised TiO_2 (Fig. 1a) was much lower than that of commercial TiO_2 (C02 and P25, Fig. 1b). The TiNT were not well-crystalline compared to the starting particles. The TiNT from sol-gel derived SiO_2-TiO_2 particles showed the highest change of crystallinity. This is probably because the presence of SiO_2 hinders crystal growth during the tube formation process. After reheating at 450°C for 2 h, the crystallinity of TiNT was slightly improved.

FTIR spectrum of SiO_2-TiO_2 particles in Fig. 2 showed broad-band adsorption of Ti-O-Ti bond (500-700 cm^{-1}), Si-O-Ti bond (960 cm^{-1}) and Si-O-Si bond (symmetric and asymmetric stretch at 800 cm^{-1} and ~1100 cm^{-1}, respectively (Ehrman and Friedlander, 1999)). The spectrum of TiNT from SiO_2-TiO_2 particles shows only the Ti-O-Ti bond but the characteristics of Si-O-Si and Si-O-Ti bonds do not appear. This can be explained that SiO_2 was dissolved in hot NaOH solution and then washed away. It is postulated that during the formation of TiNT, the bonds of Ti-O-Ti, Si-O-Si and Si-O-Ti in SiO_2-TiO_2 particles were broken to form Ti-O-Ti network. The interference of Si-O-Si and Si-O-Ti bonds during the nanotube formation led to low crystallinity of the TiNT as shown in the XRD pattern.
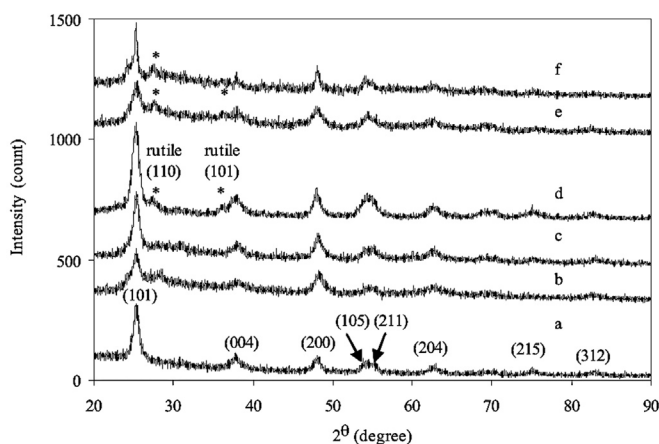

Figure 1a. XRD patterns of (a) precipitated TiO_2 nanoparticles, (b) TiNT from precipitated TiO_2 nanoparticles, (c) reheated TiNT from precipitated TiO_2 nanoparticles, (d) sol-gel derived SiO_2-TiO_2 nanoparticles, (e) TiNT from SiO_2-TiO_2 nanoparticles and (f) reheated TiNT from SiO_2-TiO_2 nanoparticles. A rutile phase was indicated by*.
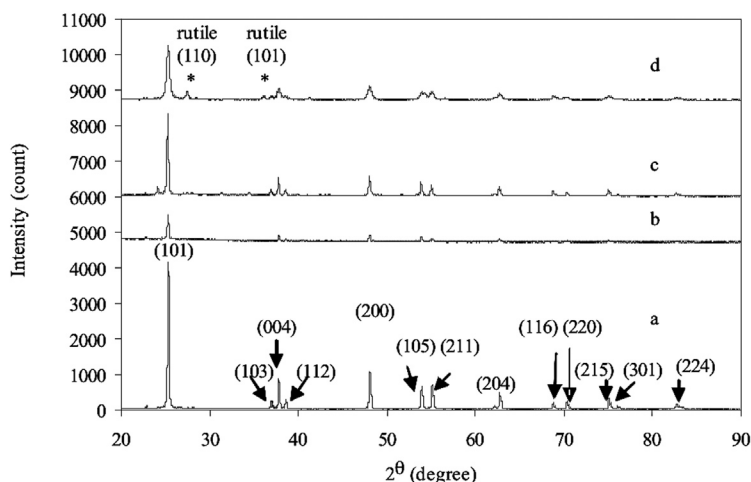
Figure 1b. XRD patterns of (a) C02 nanoparticles, (b) TiNT from C02 nanoparticles, (c) reheated TiNT from C02 nanoparticles and (d) P25 nanoparticles. A rutile phase was indicated by*
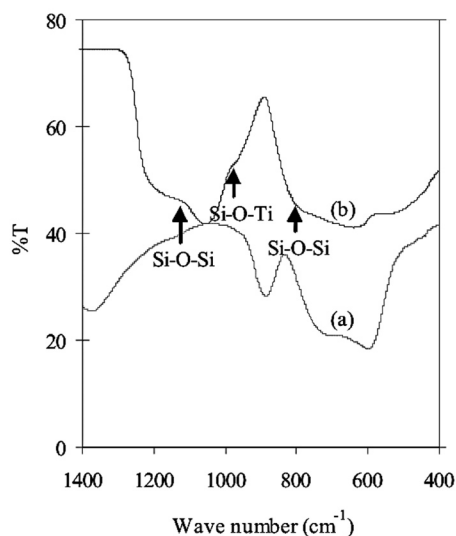

Figure 2. FTIR spectra of (a) TiNT and (b) particles of SiO_2-TiO_2. Broad adsorption bands at 500-700 cm-1 belong to Ti-O-Ti bond. Si-O-Ti bond appears at 960 cm^{-1}, and Si-O-Si bond, symmetric and asymmetric stretch, at 800 cm-1 and ~1100 cm^{-1}, respectively.

Figs. 3-5 showed the morphology of TiO_2 samples. The size and surface area are shown in Tables 1 and 2. The diameters of the nanotubes were nearly the same (~5-16 nm), regardless of the starting TiO_2 particle types. This is because the applied atmospheric pressure (in the container) during the tube formation was the same and

thus, the sizes of the tubes were in the same range (Kasuka and Hiramatzu, 1998, 2000, 2003). The length of TiNT from C02 particles was in a wide range (33-170 nm) and Fig. 5b shows agglomeration of small particles in various shapes. This is because the C02 particles, having a wide-range size (75-150 nm), were exfoliated before forming TiNT. The large particles were not completely exfoliated within the process duration, leaving the rest as small agglomerates.
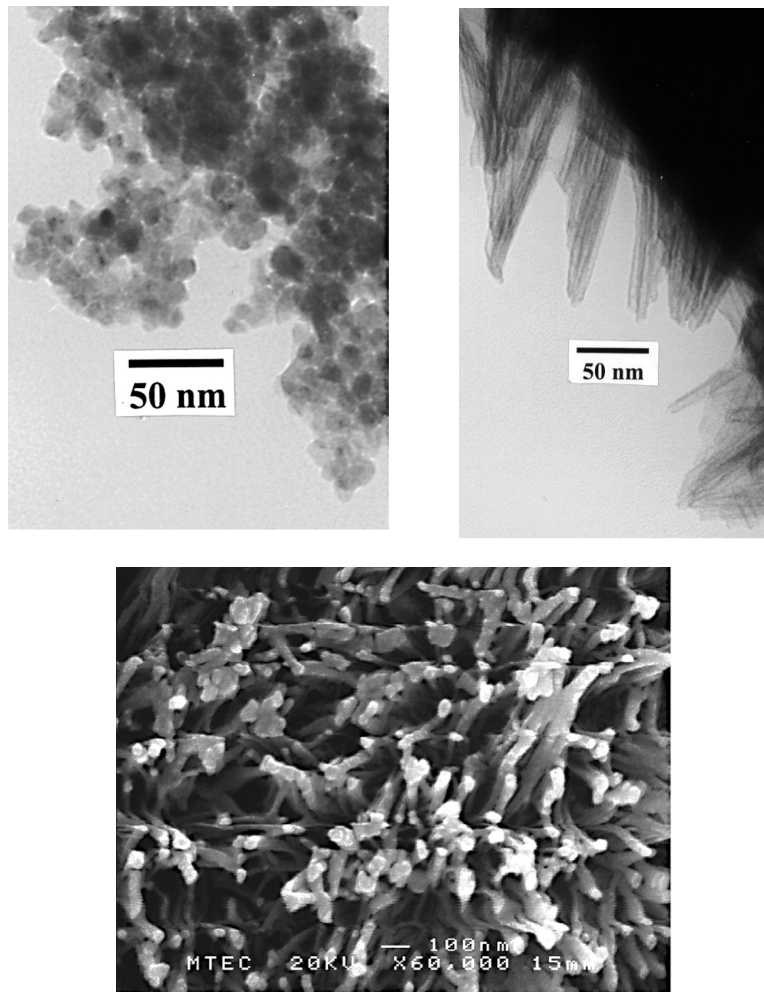

Figure 3. TEM micrographs of (a) precipitated TiO_2 nanoparticles, (b) TiNT from precipitated TiO_2 nanoparticles and (c) SEM micrograph of TiNT from precipitated TiO_2 nanoparticles.
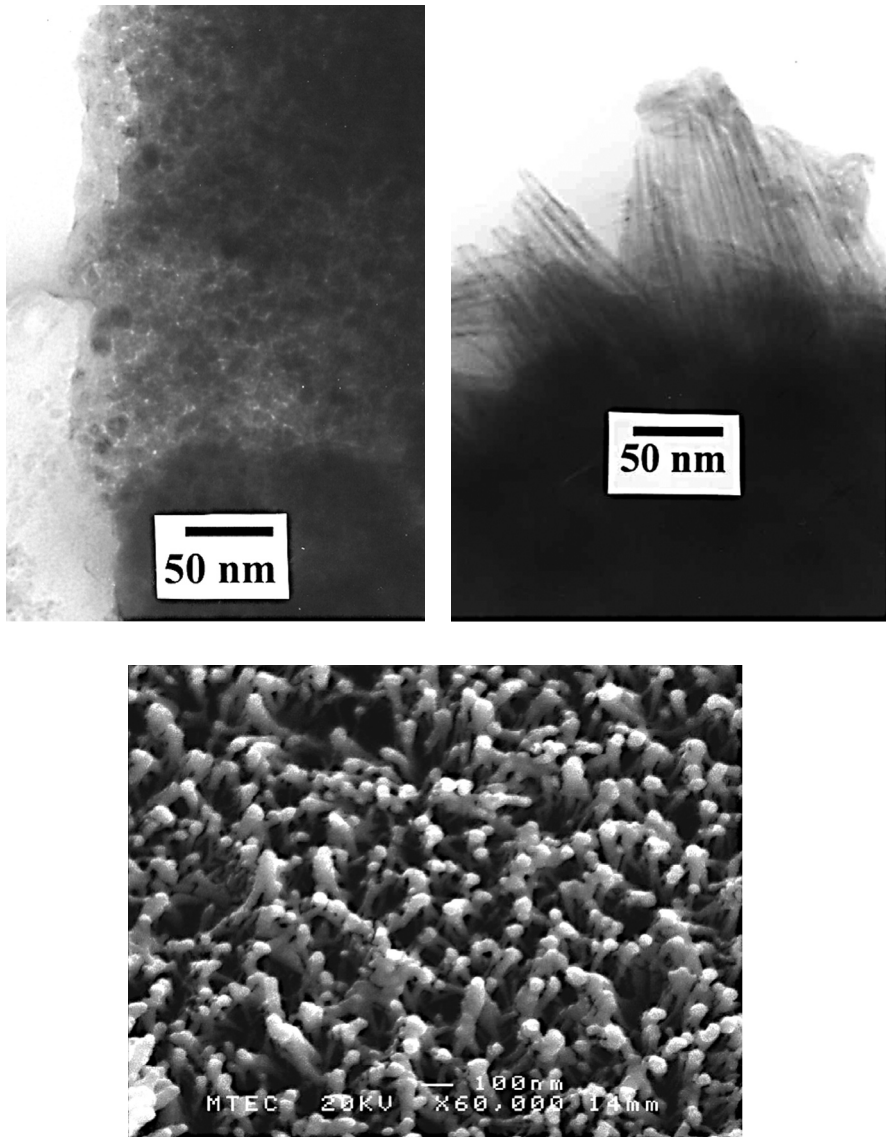
Figure 4. TEM micrographs of (a) sol-gel derived SiO_2-TiO_2 nanoparticles, (b) TiNT from SiO_2-TiO_2 nanoparticles and (c) SEM micrograph of TiNT from SiO_2-TiO_2 nanoparticles.
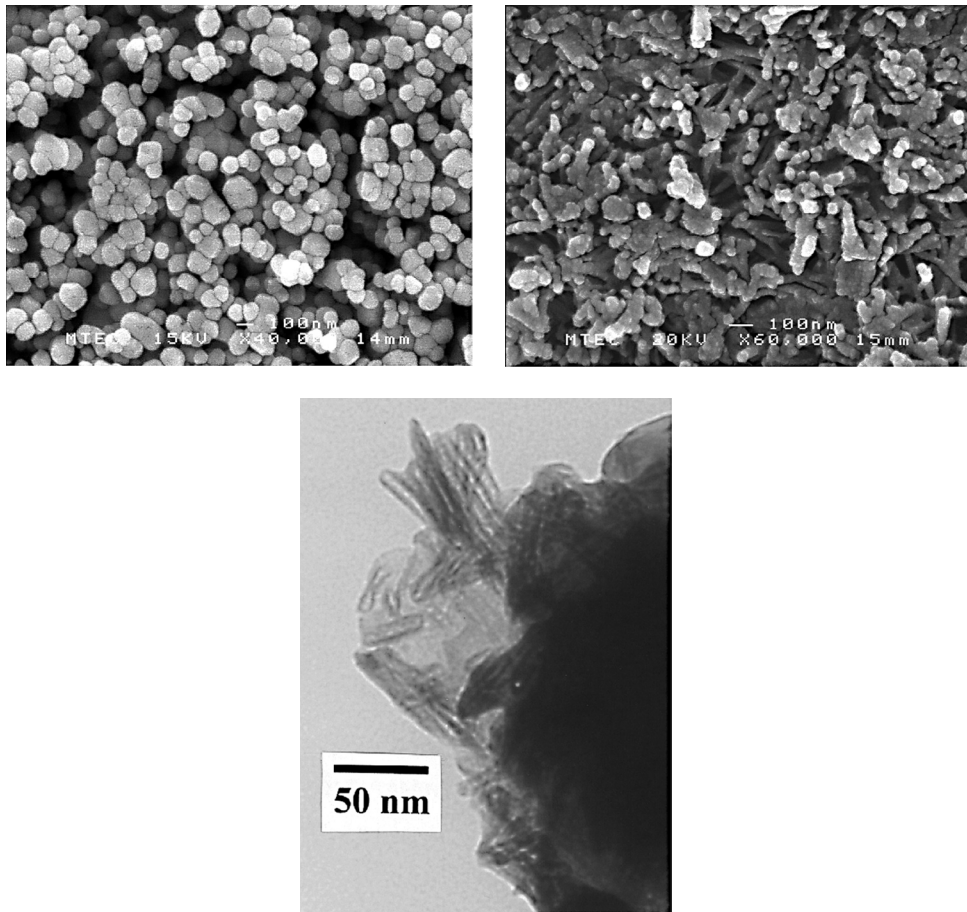
Figure 5. (a) SEM micrograph of commercial TiO_2 nanoparticles, (b) SEM micrograph and (c) TEM micrograph of TiO_2 nanotubes from commercial TiO_2 nanoparticles.

TiNT derived from the C02 particles was much smaller than their starting particles, leading to a large increase in the surface area (Tables 1 and 2). The surface area of the TiNT from precipitated TiO_2 was also higher than that of the starting particles. However, the surface area of TiNT from the SiO_2-TiO_2 was about half of that of the starting particles and half of that of the TiNT derived from other particle types. The reason for that is not clear.
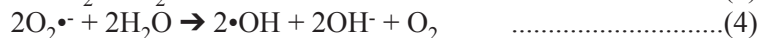
Table 1. Size and surface area of TiO_2 nanoparticles. Size was measured from SEM and TEM and surface area was measured by BET method.

Particle type	Particle size (nm)	Surface area (m² g-1)
Precipitated	4-8	127.2±2.0
SiO_2-TiO_2	5-10	199.8±2.5
C02	75-150	11.5±0.4
P25	5-37	53.6±0.7

Table 2. Size and surface area of TiNT. Size was measured from SEM and TEM and surface area was measured by BET method.

Starting TiO_2 particles	Diameter (nm)	Length (nm)	Surface area (m² g⁻¹)
Precipitated TiO_2	5-16	60-180	237.5±5.1
SiO_2-TiO_2	5-12	50-136	111.0±1.8
C02	6-10	33-170	208.6±2.7

Fig. 6 showed the time-dependent absorbance at 354 nm (the highest absorbance peaks) of the solutions, catalysed by TiO_2 samples and without catalyst. The absorbance of the solutions, at a given time, was in the order: precipitated TiO_2 particles > P25 particles > SiO_2-TiO_2 particles > TiNT from C02 particles > C02 particles > TiNT from precipitated TiO_2 particles > TiNT from SiO_2-TiO_2 particles ~ no catalyst. More I_3^- (yellow) was obtained from I^- (colorless) oxidation in the solutions having TiO_2 as catalyst because the valence band (VB) of TiO_2 (E = 2.53 V vs. SHE, Kaneko and Okura, 2002) is more positive (lower) than the reduction potential of I^-/I_3^- (E^0 = 0.536 V). The photogenerated hole in the VB was reduced by electrons from I- as shown in Equation (1). It is also possible that •OH (hydroxyl radical) created by photogenerated hole (Equation (2)) and photogenerated electron (Equations (3) and (4) (Ireland et al., 1993) oxidized I^- (Equation (5)).

$$2h^+ + 3I^- \rightarrow I_3^- \qquad\qquad ....(1)$$
$$h^+ + H_2O \rightarrow \bullet OH + H^+ \qquad\qquad ....(2)$$
$$e^- + O_2 \rightarrow O_2 \bullet^- \qquad\qquad ....(3)$$
$$2O_2 \bullet^- + 2H_2O \rightarrow 2\bullet OH + 2OH^- + O_2 \qquad ....(4)$$
$$3I^- + 2\bullet OH \rightarrow I_3^- + 2OH^- \qquad\qquad ....(5)$$

The absorbance of the solutions corresponds to photocatalytic activity of TiO_2 samples. The TiNT from precipitated TiO_2 and SiO_2-TiO_2 showed lower photocatalytic activities than their starting particles. After reheating process, the increase of photocatalytic activity of TiNT was not observed.
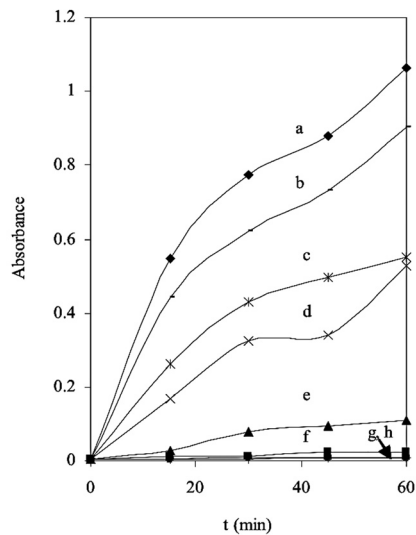
Figure 6. The time-dependent absorbance at 354 nm of the solutions catalysed by (a) precipitated TiO_2 nanoparticles, (b) P25 nanoparticles, (c) SiO_2-TiO_2 nanoparticles (d) TiNT from C02 particles (e) C02 nanoparticles, (f) TiNT from precipitated TiO_2 particles (g) TiNT from SiO_2-TiO_2 nanoparticles and (h) none.

The photocatalytic activities of TiO_2 samples related to their absorbance at 366 nm (UV light used in photocatalytic test). The absorbance of the suspensions of TiO_2 samples (5 mg in 10 ml water), shown in Fig. 7, was in the order: C02 particles > precipitated TiO_2 particles > P25 particles > TiNT from C02 particles > TiNT from precipitated TiO_2 particles > SiO_2-TiO_2 particles > TiNT from SiO_2-TiO_2 particles. The absorbance related to the amount of photons being absorbed by the TiO_2 samples and the electronic transition that could occur. TiNT showed lower absorbance than their starting particles. This is because some lattice planes in particles disappeared or became lessened in TiNT as could be seen in XRD patterns. The peak height of (004) and (200) is nearly the same for TiO_2 particles but the peak height of (004) is much lower than that of (200) for the TiNT. The peak of (101) is much higher than (200) for the TiO_2 particles but the peak of (101) is slightly higher than that of (200) for the TiNT. The change in crystallinity and the number of lattice planes affect the number of energy level and thus the electronic transition that can occur.
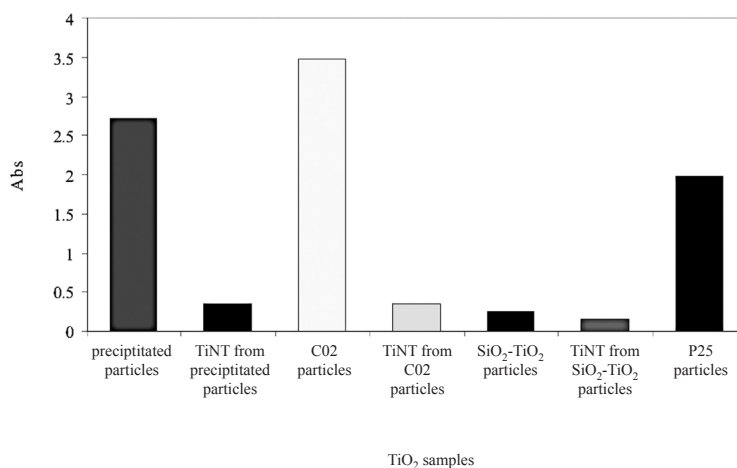
Figure 7. The absorbance at 366 nm of the TiO_2 suspensions (5 mg in 10 ml water).

The absorbance at 366 nm of SiO_2-TiO_2 particles and their TiNT was nearly the same but the former showed much higher photocatalytic activity (Fig. 6). Therefore, the lower photocatalytic activity of the nanotubes was attributed to the lower crystallinity (see XRD patterns Fig. 1) where defects in the crystal trap photogenerated holes and electrons. Since TiNT has dangling bonds and high surface energy (Tian et al., 2003; Yao et al., 2003), photogenerated holes and electrons might be trapped on the tube surface.   Moreover, the walls of TiNT were very thin compared to the particle radius, hence, photogenerated holes and electrons might recombine at the wall surface (Yang et al., 2002).

The XRD patterns of the TiNT from precipitated TiO_2 particles showed slightly lower crystallinity than their starting particles but the absorbance at 366 nm of the former was much lower than that of the latter. The surface area of the TiNT was nearly as twice as that of the particles (Tables 1 and 2). Thus, the tremendous decrease in photocatalytic activity of the TiNT, compared to the starting particles, was a result of less photon absorption. As mentioned earlier, surface defects occurring during the tube formation might trap photogenerated holes and electrons.

Adachi et al., (2003) reported that the TiNT, prepared by using a surfactant as a template, showed much higher photocatalytic activity than P25 particles. This was probably because the tubes, formed by templating technique, had a small number of surface defects compared to those formed by heating with NaOH.

The photocatalytic activity of TiNT from CO2 particles was higher than their starting particles because the surface area of the former was as nineteen times as that of the latter. It was found that small particles coexisted with TiNT (Fig. 5b). This might be the reason for the higher photocatalytic activity than the rest of TiNT. Although the absorbance at 366 nm of C02 particles was high, the fact that C02 particle is big leads to higher chance of the recombination of photogenerated holes and electrons before reaching the particle surface.

The P25 nanoparticles showed higher photocatalytic activity than most of the samples, although the surface area (53.6 m^2 g-1, determined by BET) was low, due to their high absorbance at 366 nm. Apart from C02 particles, the TiO$_2$ samples having high absorbance at 366 nm tended to show high photocatalytic activity.

TiO$_2$ suspensions absorbed different amount of UV light at 366 nm (denoted as a) and generated different amount of oxidation product at a given exposure time which was measured by absorbance at 354 nm (denoted as b). The ratios of b/a (Table 3) imply the photon-to-product conversion efficiency of the TiO$_2$ samples. The efficiency was in the order: SiO$_2$-TiO$_2$ particles > TiNT from C02 particles > P25 particles > precipitated TiO$_2$ particles > TiNT from precipitated TiO$_2$ particles ~ TiNT from SiO$_2$-TiO$_2$ particles > C02 particles. This implies that for an equal amount of absorbed photon, SiO$_2$-TiO$_2$ particles show the highest photon-to-product conversion efficiency.

Table 3. The absorbance at 366 nm of TiO$_2$ suspensions (a), absorbance of the catalysed solutions exposed to UV light of 366 nm for 30 min (b) and the ratio between absorbance of the catalysed solutions and the absorbance at 366 nm (b/a, implying the photon-to-product conversion efficiency).

Samples	Abs of TiO$_2$ suspensions (*a*)	Abs of catalysed solution (*b*)	*b/a*
Precipitated particles	2.72	0.78	0.29
TiNT from precipitated particles	0.35	0.01	0.03
C02 particles	3.48	0.08	0.02
TiNT from C02 particles	0.35	0.32	0.93
SiO$_2$-TiO$_2$ particles	0.25	0.43	1.70
TiNT from SiO$_2$-TiO$_2$ particles	0.16	0.01	0.03
P25 particles	1.98	0.61	0.31

CONCLUSION

The diameters of the TiNT were nearly the same (~5-16 nm) regardless of the types of the starting TiO$_2$ particles. The TiNT derived from the C02 particles were much smaller than their starting particles, leading to tremendous increase in surface area and photocatalytic activity. The crystallinity, the surface defects, the surface area and the photon absorptivity are important factors for photocatalytic activity. The precipitated TiO$_2$ nanoparticles showed the highest photocatlytic activity. The TiNT from SiO$_2$-TiO$_2$ particles showed the lowest photocatalytic activity. For an equal amount of absorbed photon, SiO$_2$-TiO$_2$ particles showed the highest photon-to-product conversion efficiency.

REFERENCES

Adachi, M., Y. Murata, I. Okada, and S. Yoshikawa. 2003. Formation of titania nanotubes and applications for dye-sensitized solar cells. Journal of Electrochemical Society 150: G488-G493.

Carmignani, G. M., and L. W. Frederick. 2003. US Patent 6 524 447 B1.

Ehrman S. H., and S. K. Friedlander. 1999. Phase segregation in binary SiO_2/TiO_2 and SiO_2/Fe_2O_3 nanoparticle aerosols formed in a premixed flame. Journal of Materials Research 14: 4551-4561.

Horton, I. B., and K. A. Garrett. 2002. US Patent 6 447 721 B1.

Hoyer, P. 1996. Formation of a titanium dioxide nanotube array. Langmuir 12: 1411-1413.

Ireland, C., P. Klostermann, E. W. Rice, and R. M. Clark. 1993. Inactivation of Escherichia coli titanium dioxide photocatalytic oxidation. Applied Environmental Microbiology 59: 1668-1670.

Jung, J. H., H. Kobayshi, K. J. C. V. Bommel, S. Shinkai, and T. Shimizu. 2002. Creation of novel helical ribbon and double-layered nanotube TiO_2 structures using an organogel template. Chemistry of Materials 14: 1445-1447.

Kaneko, M., and I. Okura. 2002. Photocatalysis, Science and Technology. Kodansha Springer. Japan

Kasuga, T., M. Hiramatsu, A. Hoson, T. Sekino, and K. Niihara. 1998. Formation of titanium oxide nanotube. Langmuir 14: 3160-3163.

Kasuka, T., and M. Hiramatsu. 1998. JP Patent 10152323.

Kasuga, T., and M. Hiramatsu. 2000. US Patent 6 027 775.

Kasuga, T., and M. Hiramatsu. 2003. US Patent 6 537 517 B1.

Kay, A., and M. Gratzel. 1996. Low-cost photovoltaic modules based on dye-sensitized nanocrystalline titanium dioxide and carbon powder. Solar Energy Materials and Solar Cells 44: 99-117.

Tian, Z. R., J. A. Voigt, J. Liu, B. Mckenzie, and H. Xu. 2003. Large oriented arrays and continuous films on TiO_2-base nanotubes. Journal of the American Chemical Society 125: 12384-12385.

Wilke, K., and H. D. Breuer. 1999. The influence of transition metal doping on the physical and photocatalytic properties of titania. Journal of Photochemistry and Photobiology A: Chemistry 121: 49-53.

Xu, J. C., M. Lu, X. Y. Guo, and H. L. Li. 2005. Zinc ions surface-doped titanium dioxide nanotubes and its photocatalysis activity for degradation of methyl orange in water. Journal of Molecular Catalysis A: Chemical 226: 123-127.

Yang, P., C. Lu, N. Hua, and Y. Du. 2002. Titanium dioxide nanoparticles co-doped with Fe3+ and Eu3+ ions for photocatalysis. Materials Letters 57: 794-801.

Yao, B. D., Y. F. Chan, X. Y. Zhang, W. F. Zhang, Z. Y. Yang, and N. Wang. 2003. Formation mechanism of TiO_2 nanotubes. Applied Physics Letters 82: 281-283.

Zhang, Y., and A. Reller. 2002. Nanotubes in Si-doped titanium dioxide. Chemical Communications 6: 606-607.